PERGAMON

International Journal of Solids and Structures 37 (2000) 3715–3732

INTERNATIONAL JOURNAL OF SOLIDS and STRUCTURES

www.elsevier.com/locate/ijsolstr

Experimental investigation of the quasi-static fracture of functionally graded materials

H. Li, J. Lambros*, B.A. Cheeseman, M.H. Santare

Mechanical Engineering Department, University of Delaware, Newark, DE 19716, USA

Received 31 August 1998; received in revised form 1 February 1999

Abstract

In this paper we describe the fracture testing of model Functionally Graded Materials (FGMs). The FGMs were created by selective ultraviolet (UV) irradiation of a polymer. An ethylene carbon monoxide copolymer (ECO) was chosen to make the specimen because of its rapid degradation under UV light. ECO becomes stiffer, stronger and more brittle with increasing irradiation time. By controlling exposure time we produced specimens with continuously varying mechanical properties. We conducted single edge notch fracture tests on both homogeneously irradiated ECO and functionally graded ECO. A hybrid numerical-experimental method was used to evaluate fracture parameters. The stress versus crack length relation, obtained experimentally, was used as the boundary conditions at each increment of crack growth in a Finite Element Analysis (FEA). From the FEA we calculated the *J*-integral, energy release rate and stress intensity factor for 5-, 60- and 106-h uniformly irradiated ECO, as well as for several FGMs. The fracture toughness of homogeneously irradiated ECO showed a rise following initiation and then remained constant during crack growth. The magnitude of the fracture toughness decreased with increasing irradiation time. For the case of FGMs it was observed that fracture toughness increased throughout crack growth (i.e. did not reach a plateau) when the crack propagated from the stiffer to the more compliant region.

Keywords: Functionally graded material; Fracture; Resistance curve; ECO; Polyethylene; UV irradiation

1. Introduction

Functionally Graded Materials (FGMs) are inhomogeneous materials which are tailored in such a way as to derive beneficial behavior from their inhomogeneity. FGMs were first developed in ceramic thermal coatings to overcome the problems originating when a ceramic layer was bonded to a metal

* Corresponding author. Tel.: +1-302-831-1147; fax: +1-302-831-3619.
E-mail address: lambros@me.udel.edu (J. Lambros).

0020-7683/00/$ - see front matter
PII: S0020-7683(99)00056-6

substrate. The introduction of FGMs allowed the synthesis of a coating that contains no ceramic at the interface and gradually increases to 100% ceramic at the free surface (Erdogan, 1995). Limitations on the use of FGMs have arisen primarily from the lack of understanding of the fracture behavior of such inhomogeneous materials.

There has been almost no experimental research on the topic of fracture mechanics of nonhomogeneous materials. In contrast to this, there is a growing body of theoretical work published on the topic. Without attempting an exhaustive review of this work, we will point out and discuss several important studies and results relevant to the present research. There are several papers which address the behavior of a straight crack in an infinitely extended continuously nonhomogeneous material (CNM). In particular, Delale and Erdogan (1983), solved the Mode I problem for the crack in an unbounded CNM. The material properties varied in the direction parallel to the crack allowing for a purely symmetric solution. Gerasoulis and Srivastav (1980), solved a related problem where the property variation was in the direction perpendicular to the crack. But in their solution, they also imposed symmetry by assuming the property gradient was symmetric about the plane of the crack. Both these studies showed that the stress intensity factor can be significantly affected by the degree of nonhomogeneity. The general in-plane mixed-mode problem was solved by Konda and Erdogan (1994). In this study, they tabulate a large number of mode I and mode II stress intensity factors for a variety of crack-nonhomogeneity orientations under several different load cases.

Also of great theoretical and practical interest are solutions for the crack at or near an interface between a CNM and a homogeneous material (e.g. Delale and Erdogan, 1988a, b). One interesting result of these studies is the observation that, due to the lack of symmetry, the crack tip stresses are inherently mixed mode. Therefore the propagating crack would tend to kink or curve in these situations. Other studies focus on cracks perpendicular to discrete interfaces between dissimilar CNMs and between CNMs and homogeneous materials (Choi, 1996; Gao and Kuang, 1992).

Atkinson and List (1978), consider a steady state crack propagating in a nonhomogeneous material. In their study, the crack grows in the direction of the nonhomogeneity and therefore crack propagation is purely self-similar. Although there are a number of restrictive assumptions used in the study, it is unique in that it is the only one which examines crack propagation in CNMs.

Some of the early studies (e.g. Delale and Erdogan, 1983) concluded that the effect of Poisson's ratio on the fracture response of an FGM was negligible. Thus, in most subsequent studies Poisson's ratio was assumed a constant and only Young's modulus was allowed to vary. However, in all theoretical studies the modulus of elasticity was assumed to vary exponentially according to the relationship,

$$E(x, y) = E_0 \, \mathrm{e}^{(\beta x + \gamma y)}. \tag{1}$$

In this relationship, E is the modulus of elasticity, x and y are spatial coordinates and E_0, β and γ are constants which determine the shape of the nonhomogeneity function. This assumption is used to facilitate the solution procedure by reducing the governing equation for the Airy's stress potential to a fourth order PDE with constant coefficients. Jin and Noda (1994) show, however, that the asymptotic square root singularity and the angular distribution of the elastic stresses are identical to those in the homogeneous case as long as the nonhomogeneity function for the properties of the region in which the crack tip resides is continuous and piecewise differentiable.

Of particular interest to the present study is the work of Erdogan and Wu (1997). They studied the edge crack problem for a plate with functionally graded properties subjected to several types of in-plane loading. They also used a constant Poisson's ratio and a Young's modulus exponentially varying from one end of the plate to the other end. Results were presented as the normalized plane-strain stress

intensity factors for different material nonhomogeneity parameter β. [In eqn (1) γ was assumed to be zero.] A combination of the fixed grip loading and bending boundary conditions studied by Erdogan and Wu (1997) in plane-strain deformation, is very similar to our experimental study, described in the following sections, with the exception that our experiments are essentially under plane-stress conditions.

Jin and Batra (1996) employed a crack-bridging concept and the rule of mixtures method to study the fracture behavior of a ceramic–metal FGM with an edge crack. The crack bridging concept can be used to study the toughness, or R-curve behavior, of an FGM when it is fabricated with the metal having relatively large grains and the ceramic having smaller grains. The rule of mixtures method was used to scale the fracture toughness of the FGM by the volume fraction of its constituents. They concluded that the fracture toughness of their FGM significantly increases when a crack grows from the ceramic-rich region into the metal-rich region, i.e. from the brittle to the ductile zone.

Although numerous such theoretical models exist, their verification has not been possible because of lack of experimental data regarding the fracture of FGMs. The primary reason behind this is the difficulty of fabricating laboratory scale FGMs. Many ways of fabricating FGMs have been developed (e.g., powder processing, thermal spraying, chemical and physical vapor deposition, combustion synthesis, diffusion treatments, and sedimentation—see Rabin and Shiota, 1995 for a review). However, all these methods suffer from common problems of high equipment and material costs and small resulting product size. For these reasons the methods may not be practical for providing specimens for an experimental investigation of the bulk properties of FGMs. In addition, their inherently layered structure does not allow detailed study of the fracture behavior based only on material nonhomogeneity, since the layering will also effect the fracture characteristics of the material.

Lambros et al. (1999) have developed a method, based on selective UV irradiation of polymers, for economical fabrication of laboratory scale FGMs. In the present paper, we discuss results of an experimental study of the fracture behavior of these FGMs. The material used in the fabrication of model FGMs is ECO, an abbreviation of polyethylene co-carbon monoxide. The ECO sheet used in this study contains 1 wt% carbon monoxide. It is commercially available from Hi-Cone Division, Illinois Tools Works, Co., Chicago, who kindly donated it for this work. The advantage of using this method for manufacturing the FGM is that the resulting material will be truly continuously nonhomogeneous.

It is well known that polyethylene based materials undergo a change of mechanical properties when subjected to UV irradiation (Li and Guillet, 1980; Ivanova et al., 1996; Lambros et al., 1999). This is especially true for ECO, which has been designed specifically to be susceptible to UV light. Although the tensile behavior of irradiated ECO has been well documented (Andrady and Nakatsuka, 1994; Ivanova et al., 1996; Lambros et al., 1999), the effects of UV irradiation on the fracture behavior of ECO have not been studied extensively. To our knowledge, the only studies dealing with the subject are those of Ivanova et al. (1995, 1996). Ivanova et al. (1995) studied the effects of UV irradiation on the fatigue behavior of ECO specimens. Their results showed that the fatigue fracture lifetime in single edge notch specimens was reduced by a factor of 10 after a UV irradiation time of about 20 h. They concluded that the reduction of fatigue lifetime is associated with reduction in the process zone size and decreases in the ductility of the fracture surface. They also presented the results of their study on the effects of UV radiation on crack initiation and crack growth speed. Also, Ivanova et al. (1996) developed a technique to model crack propagation in a discretely heterogeneous material by selectively photodegrading the same ECO film.

In the present paper we present the results of an experimental study into the fracture behavior of a model FGM. First a thorough study of fracture behavior of irradiated ECO is presented in Section 2. The fracture behavior of the model FGMs is then presented in Section 3.

2. Fracture behavior of ECO

2.1. Experimental set-up

We studied the Mode I fracture behavior of homogeneously irradiated ECO by a hybrid experimental-numerical method. The specimen geometry used in the fracture experiments was a single edge notch specimen shown in Fig. 1. The dimensions of the fracture test specimen are $W = 150$ mm, $H = 100$ mm and the thickness $t = 0.42$ mm. Since the dimensions of width and height of the specimen are far greater than the thickness, we model the test as plane-stress. The initial length of the edge crack is $a_0 = 30$ mm. The loading mechanism, also illustrated in Fig. 1, consisted four metal rings linking the specimen end tabs to metal bars at each side. The load was then applied at the midpoints of the metal bars.

A schematic of the experimental set-up for the testing of the fracture specimens is shown in Fig. 2. We used a Tektronix TDS 540B Digitizing Oscilloscope to record the force exerted by the Instron machine. Since we used a fixed crosshead speed, this data can be easily converted to a load-displacement relation. In parallel, we used a Sony XC-77 CCD camera and a Sanyo TLS-7000 VCR to record the crack initiation and growth events. The video signal was then digitized using an Indigo II SGI computer. Such a setup allows for image collection at a rate of 60 frames/s, which provides sufficient temporal resolution to record quasi-static crack growth. The appropriate images are used to measure the crack length and calculate its growth rate.

A selected sequence of four frames recorded by the CCD camera is shown in Fig. 3. The scale in each

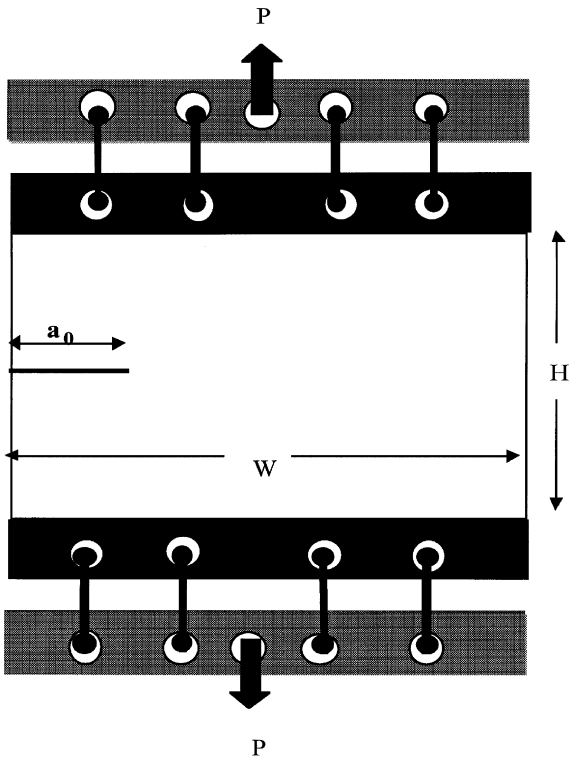

Fig. 1. Geometry and loading of single edge notch fracture specimen.

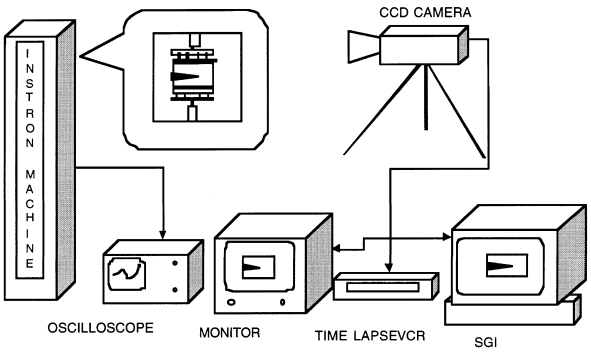

Fig. 2. Schematic of experimental set-up in fracture testing of ECO.

frame, consisting of a transparent ruler, allows measurement of the crack length. The clock on the VCR provides a record of time. In this fashion, we can obtain the variation of crack length with time. By synchronizing the load recording oscilloscope and VCR time bases, we can deduce a load versus crack length curve. This curve, a typical example of which is shown in Fig. 4, represents the main result sought from this experiment. The data in the load versus crack length curve can then be used, with a finite element model, to calculate fracture parameters as described in the next section.

2.2. Finite Element Analysis

Finite Element Analysis of the edge crack problem was conducted using the FEA software packages PATRAN (MacNeal-Schwendler Corporation, PATRAN Version 5.0) and ABAQUS (Hibbit, Karlsson and Sorensen, Inc., ABAQUS Version 5.4-1). In these experiments the crack propagates through the

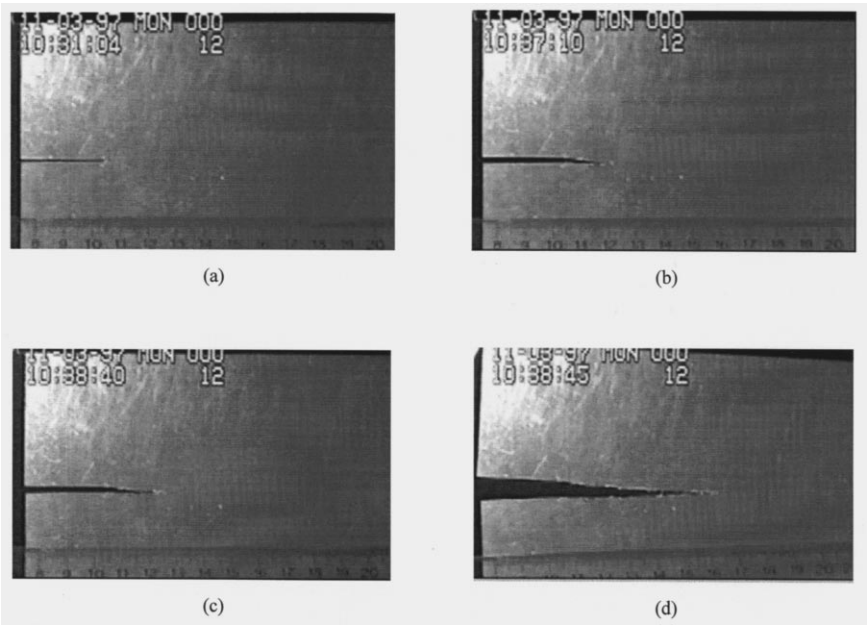

Fig. 3. Selected sequence of CCD frames showing quasi-static crack growth in 5-h UV irradiated ECO.

midline of the specimen. Thus, because of symmetry, we modeled only half of the test specimen. Since the loading on the specimen produced by the self-aligning fixture illustrated in Fig. 1 is quite complex, we chose to simulate the loading fixture as well as the specimen. The mesh used for the specimen and fixture is shown in Fig. 5. All linkages are assumed to be rigid truss elements. We used eight noded quadrilateral plane-stress elements and refined the mesh near the crack tip area as shown in the figure. We fixed the displacement in y-direction on the specimen centerline nodes ($y = 0$) but left the crack surface nodes free. To avoid rigid body translation of the model, the end node on the centerline opposite the crack was fully constrained. The experimentally measured load corresponding to each measured crack length was then imposed as the boundary condition at the top most linkage bar. This hybrid method of analysis can be used only up to the point at which the crack length reached about 65 mm. After this crack length, significant compressive stress is generated in the ligament area across from the crack tip which can lead to buckling. This effect corresponds to wrinkling of the sheet, seen in the later stages of the experiments.

Despite the fact that the ECO material shows some plastic behavior, as a starting point we attempted to model the material behavior as homogeneous linear elastic. This assumption is better justified for the longer irradiation times (Lambros et al., 1999). However, during and after testing, plasticity effects near the tip were clearly visible. It is believed that these are confined to a small region near the crack tip. From the load record in Fig. 4, we can deduce that typical values of the maximum applied stress attained during the fracture experiment are about 50% of the yield stress of ECO which has been subjected to low amounts of irradiation (i.e. less than 30 h). In addition, for longer UV irradiation times, over about 40 h, the ECO material becomes essentially brittle. Therefore, in all cases except for the most ductile ones (<2 h irradiation) conditions of small scale yielding are assumed to occur. This point is further discussed in Section 2.4.

For linear elastic material behavior it is well known that the stress directly ahead of the crack tip asymptotically approaches

$$\sigma_{yy} = \frac{K_{\mathrm{I}}}{\sqrt{2\pi r}}, \tag{2}$$

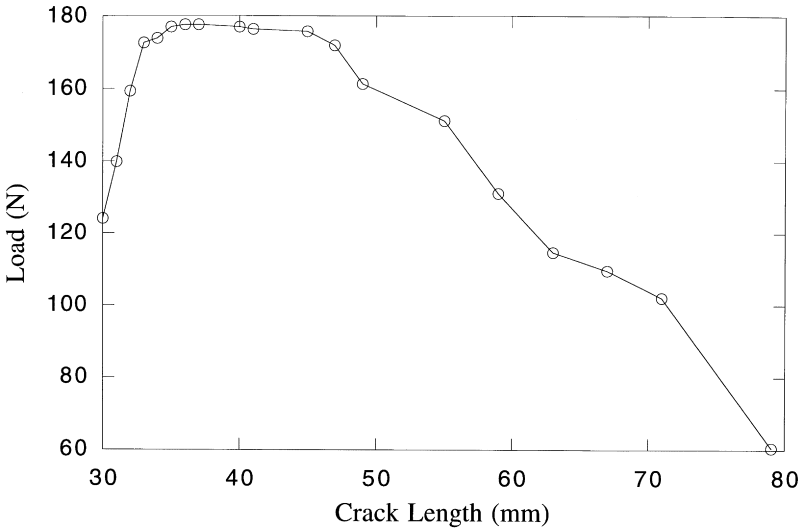

Fig. 4. Experimentally measured load versus crack length relation for 5-h uniformly irradiated ECO edge crack specimen.

as r becomes smaller, where K_I is the Mode-I stress intensity factor and r is the distance ahead of the tip. Since plane-stress small scale yielding conditions will be assumed, the stress intensity factor K_I can be easily related to the energy release rate G and the J-integral through

$$J = G = \frac{K_I^2}{E}, \tag{3}$$

where E is the Young's modulus of the homogeneous material. Both G and J can be computed from the finite element calculations; the former using a node release technique, the later using the domain integral technique. A mesh sensitivity study was conducted to determine the optimal element size and crack extension for the computation of G and J. This study also showed that J and G are indeed equal, in the purely elastic case.

2.3. Results for fracture of homogeneous ECO

In the present work we use the experimentally recorded load versus crack length relation (Fig. 4) to calculate the history of G for each particular fracture specimen. The FEA model is run at a series of time intervals with the known crack length and applied load. For each of these configurations the

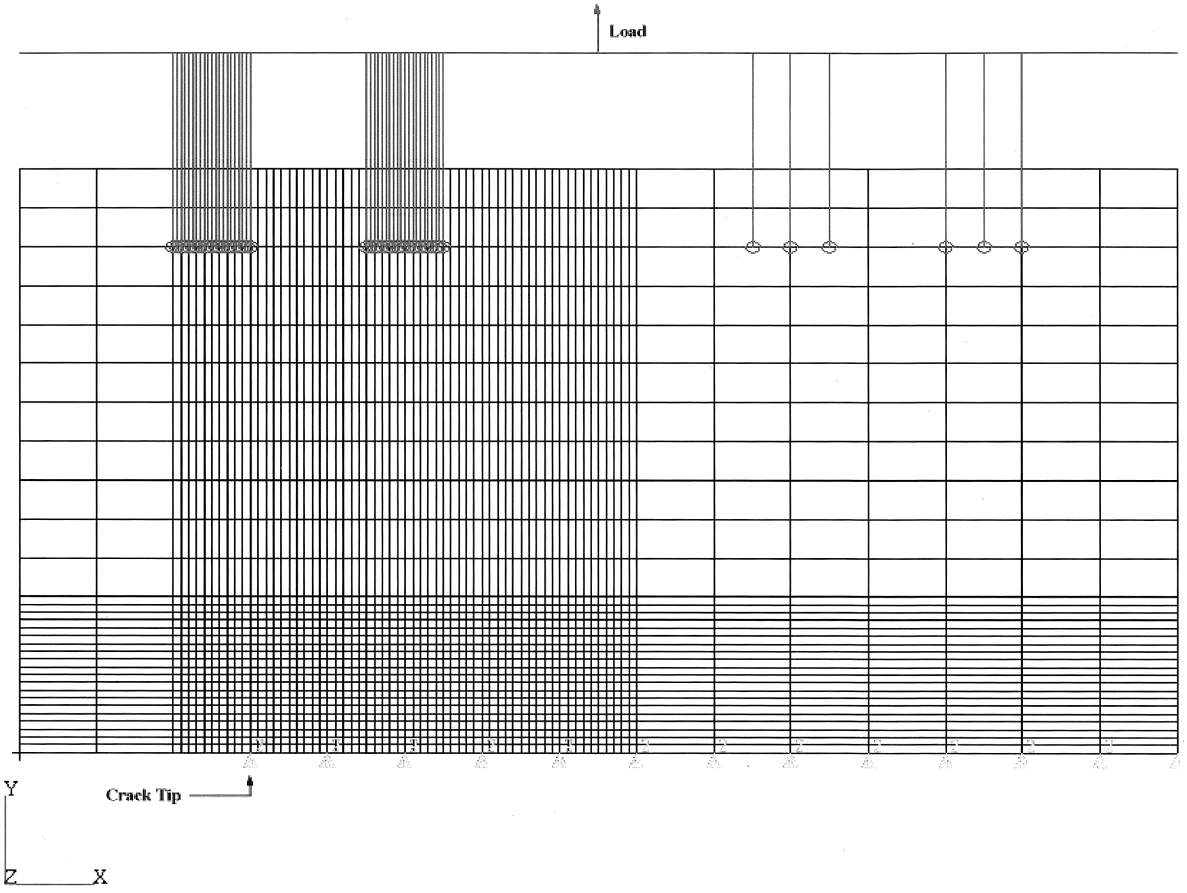

Fig. 5. Mesh used in the FEA model of the edge crack test.

resulting energy release rate is determined. In this way, we can calculate the G for the entire crack development. Fig. 6 shows the energy release rate G for fracture specimens of 5-, 60- and 106-h uniformly irradiated ECO. We see that G increases after crack initiation, but as irradiation time increases the values of G for a given crack length decrease. In addition, the slope of the G–a curve also decreases with increasing irradiation time, because of a decrease in near tip ductility.

Although the material has been modeled as linear elastic, a resistance-type behavior of its toughness versus crack length is observed. This occurs because locally there are plasticity effects near the crack tip, where a stress concentration exists. If plasticity is confined to small scale yielding conditions, however, evaluation of G in the manner described is still valid. Under such conditions we can also obtain the variation of K_I through the use of eqn (3). A plot of these results is shown in Fig. 7. In addition, a decrease of the initiation toughness was observed with increasing irradiation time ($K_{IC} = 0.682$, 0.644, 0.607 MPa$\sqrt{}$m for the 5-, 60- and 106-h irradiated ECO respectively).

2.4. Limitations and errors of the technique

There are several limitations to the above method for obtaining the stress intensity factor K_I and the energy release rate G. In this section we will briefly address the most important ones.

2.4.1. Non-linear material behavior

Both non-irradiated and irradiated ECO show distinctly nonlinear behaviors for the strain rates employed in this study (Lambros et al., 1998). However, the non-linearity dramatically decreases with increasing irradiation time. This nonlinear material behavior may be attributed to either non-linear elastic or plastic effects. Fig. 8 shows a loading–unloading stress–strain curve for a 55-h irradiated ECO material. A maximum stress level of 5 MPa was applied yet the material shows little residual plastic strain. It does, however, exhibit substantial non-linear and viscoelastic behavior. Such behavior becomes

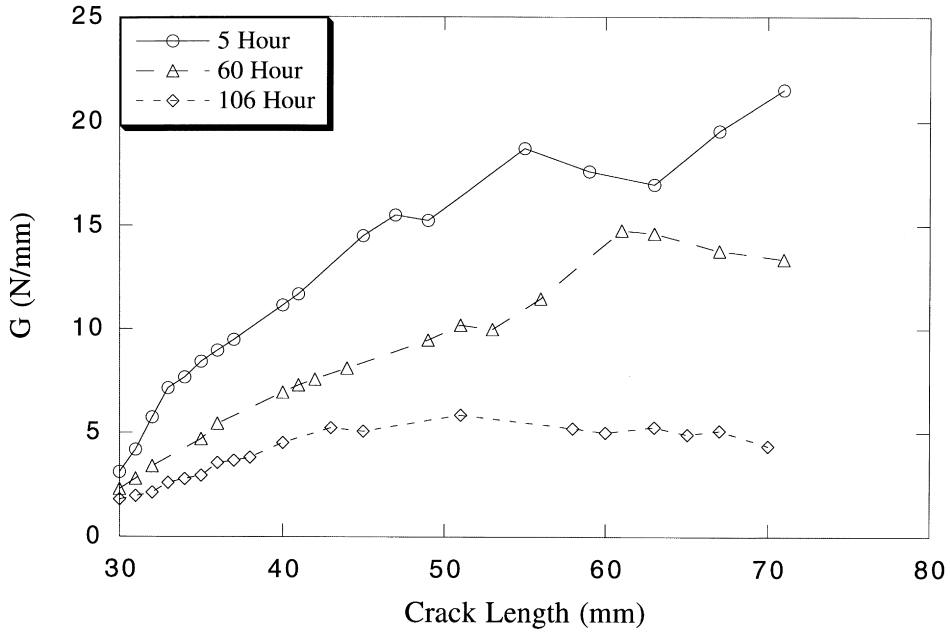

Fig. 6. Resistance curve based on G for edge crack specimen of ECO at three different irradiation times, 5-, 60- and 106-h.

less pronounced as irradiation time increases, since the material becomes more brittle. This is the case for most of the fracture experiments. In addition, all fracture experiments were conducted over relatively short time frames ($\approx$100–250 s), i.e. time frames which also diminish the importance of any viscoelastic effects. Thus, there is some evidence that the assumption of linear elasticity in the fracture experiments is reasonable, especially for the longer irradiation times.

To confirm the extent of the nonlinear zone, a nonlinear finite element analysis was conducted for a typical scenario in the fracture experiments conducted. Given the measured tensile stress–strain data for the 60-h irradiated ECO, an incompressible power law hardening behavior was assumed. (Note that the assumption of incompressibility is well justified for polyethylene.) The elastic potential, W, fitted to the tensile stress–strain experimental data was taken to be

$$W(I_1, I_2) = \sum_{i+j=1}^{2} C_{ij}(I_1 - 3)^i (I_2 - 3)^j, \tag{4}$$

where C_{ij}, are material parameters, and I_1 and I_2 the first and second invariants of the Green's strain tensor, respectively. The experimentally obtained geometry and loading shown in Fig. 4 were again used, but this time in a non-linear FEA framework. It was then possible to determine the extent of non-linearity near the crack tip by comparing the results of the non-linear and linear FEA. The quantity used in comparing the two solutions was the ratio (Rosakis and Rosakis, 1988),

$$e_1 = \frac{\|\sigma^{\mathrm{NL}}_{\alpha\beta} - \sigma^{\mathrm{L}}_{\alpha\beta}\|}{\|\sigma^{\mathrm{L}}_{\alpha\beta}\|}, \tag{5}$$

where $\sigma^{\mathrm{NL}}_{\alpha\beta}$ are the components of stress determined by the non-linear analysis, $\sigma^{\mathrm{L}}_{\alpha\beta}$ are those determined by the linear analysis and $\|\|$ denotes the norm of the tensor. Fig. 9 shows a contour plot of the

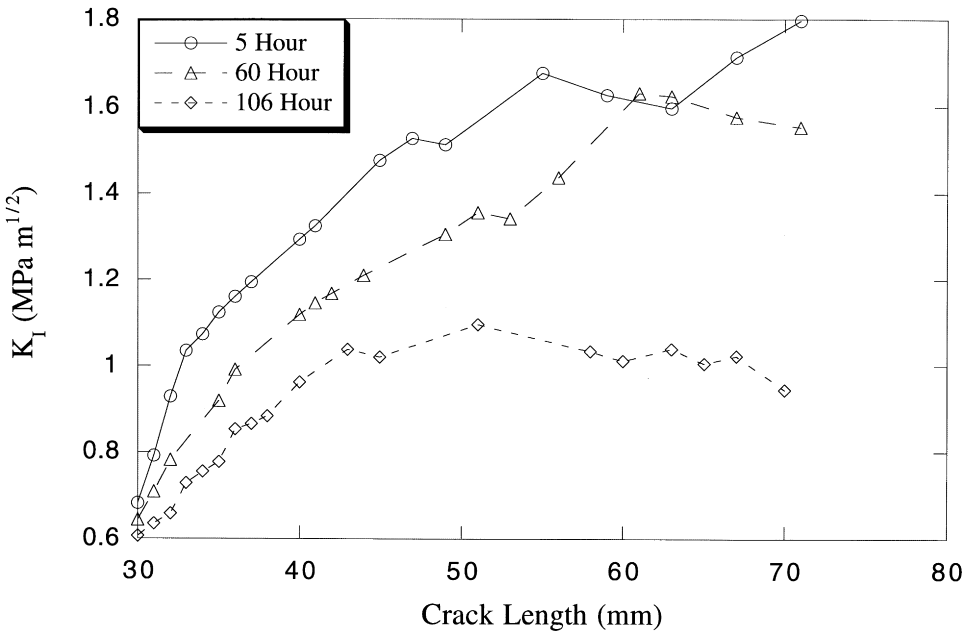

Fig. 7. Resistance curve based on K_I for edge crack specimen of ECO at different irradiation times, 5-, 60- and 106-h.

quantity e_1 for the case a 60-h, uniformly irradiated ECO sample with a 30 mm crack length at the instant of crack initiation. It is clear from this figure that the scale of the non-linear effect is localized near the crack tip. (The size of each 8-noded quad element used in the FEA was 1 mm.) A difference of 20% between the linear and non-linear cases extends only up to about 3 mm around the crack tip. Thus, the use of a linear elastic material assumption provides a reasonable approximation.

2.4.2. K-dominance

A *K*-dominant region is defined as one in which the crack tip stresses are well approximated by the leading term of the asymptotic expansion. In eqn (2) for K_I to have physical significance, a substantial *K*-dominant region must exist in the specimen under observation. Strictly speaking, before quoting values of K_I, this assumption should be verified using either near tip measurements or an indirect numerical analysis. In the future it is planned to extend this experimentation using near-tip, full-field measurements. For the present study the results of the elastic numerical simulation of the fracture specimen were used to estimate the extent of *K*-dominance. This was determined by looking at the quantity.

$$e_2 = \frac{\|\sigma_{\alpha\beta}^{2\text{-D}} - \sigma_{\alpha\beta}^{K}\|}{\|\sigma_{\alpha\beta}^{K}\|}$$

where $\sigma_{\alpha\beta}^{2\text{-D}}$ denotes the two-dimensional plane-stress numerical results and $\sigma_{\alpha\beta}^{K}$ denote the stresses obtained by the *K*-dominant stress field [eqn (2)] using the value of K_I obtained from the node release procedure (Fig. 7). Figs. 10(a) and (b) show contours of the quantity e_2 for an experiment on a 60-h uniformly irradiated material with the loads corresponding to a 30 mm crack (i.e. crack initiation) and a 44 mm crack, respectively. As can be seen in Fig. 10(a) a substantial region of *K*-dominance exists around the tip. For example, the 6% error contour extends 15 mm around the tip. As crack length increases, Fig. 10(b), the region of *K*-dominance decreases in size. However, it still occupies a substantial part of the near-tip region. It is therefore meaningful in this problem to quote values of stress intensity

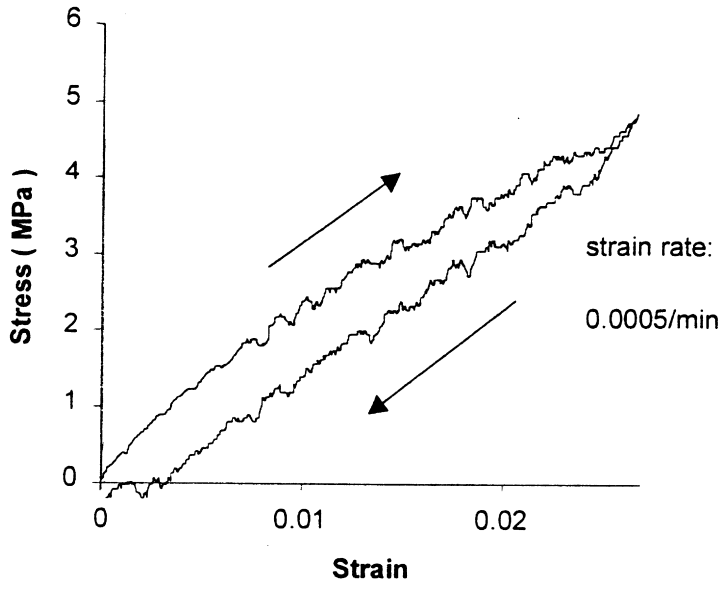

Fig. 8. Loading–unloading stress–strain curve for 55-h irradiated ECO.

factor K_I. Note that even if K-dominance does not exist, this would not affect the validity of the fracture parameters G or J which are energy related quantities measured for the specimen as a whole.

2.4.3. Poisson's ratio

From the literature (Domininghaus, 1993), we find the Poisson's ratio of low density Polyethylene (LDPE) to be about 0.45. However, the effect of UV radiation on it is unknown. In the uniaxial tension test, we attempted to measure Poisson's ratio of ECO using strain gages and an LVDT (Linear Variable Differential Transformer). Because of the nature of the ECO specimens, both methods were unsuccessful. Existing theoretical studies of the fracture of FGMs have shown that Poisson's ratio does not influence the results very much (Delhale and Erdogan, 1983). In addition, we performed our own parametric study by varying the Poisson's ratio used in the FEA between 0.3 and 0.45. The difference in results was negligible (less than 1%). Thus, in all further work we used a value of 0.45, the nominal Poisson's ratio of LDPE.

2.4.4. Initiation time

An error is introduced in the measurement of the initiation value of the fracture toughness, K_{IC}, through the uncertainty of determining the exact crack initiation time. Two sources are the main contributions to the initiation time error: (a) synchronization of force and crack length measurements, (b) precise determination of the image corresponding to crack initiation. Applied force is continuously recorded on a digital storing oscilloscope. Crack initiation and growth is imaged on a VCR. Each of the

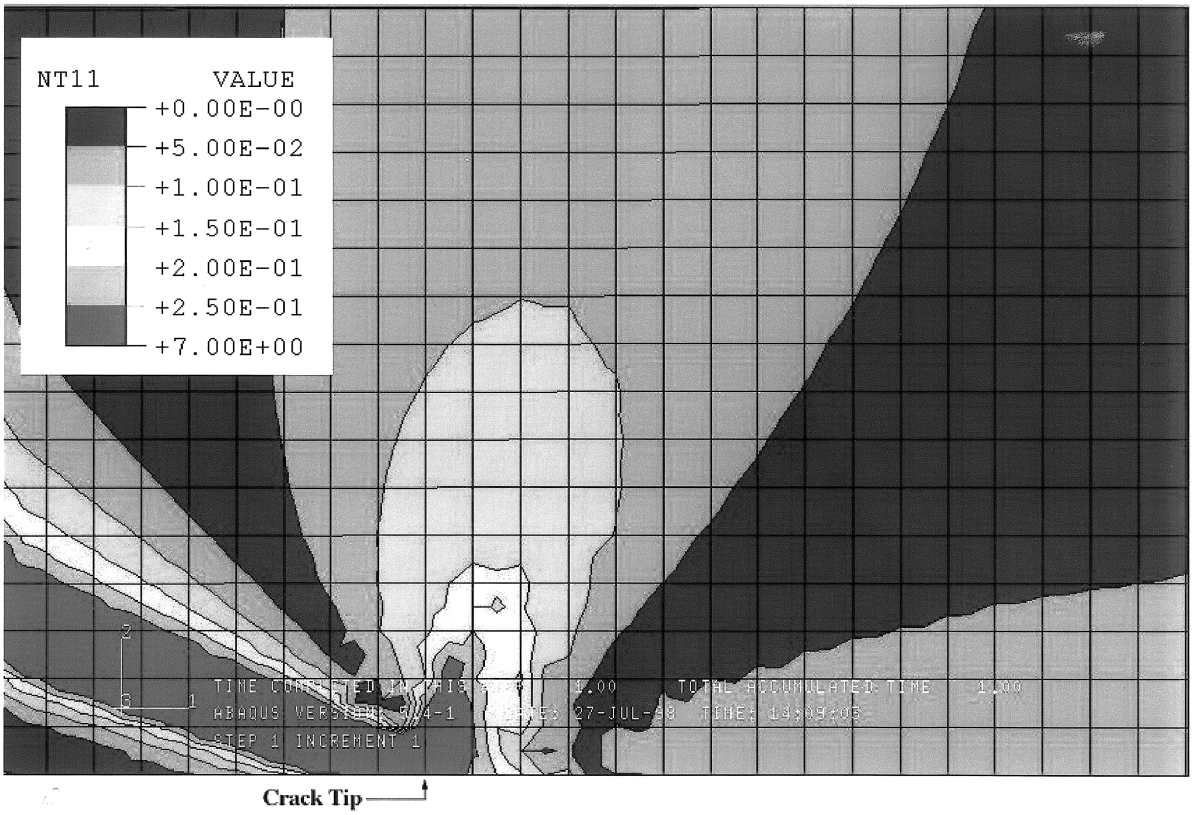

Fig. 9. Extent of non-linear zone, as determined by the quantity e_1, at the instant of crack intiation in 60-h irradiated ECO fracture experiment.

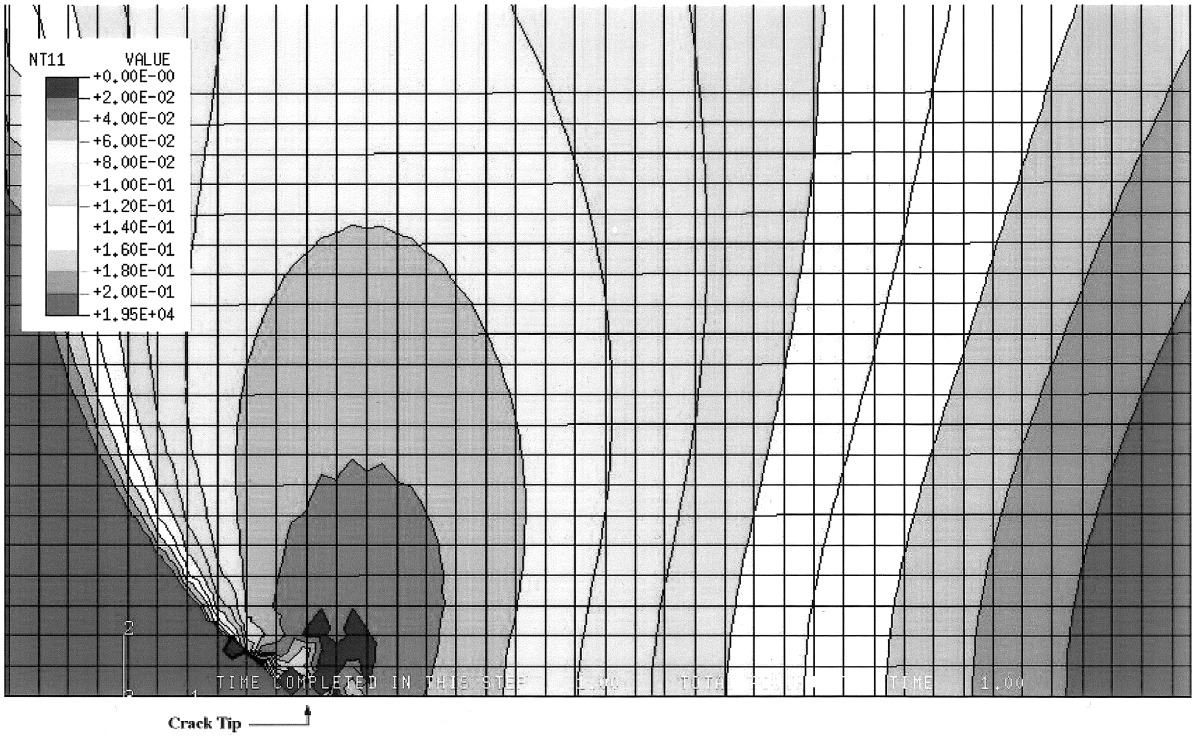

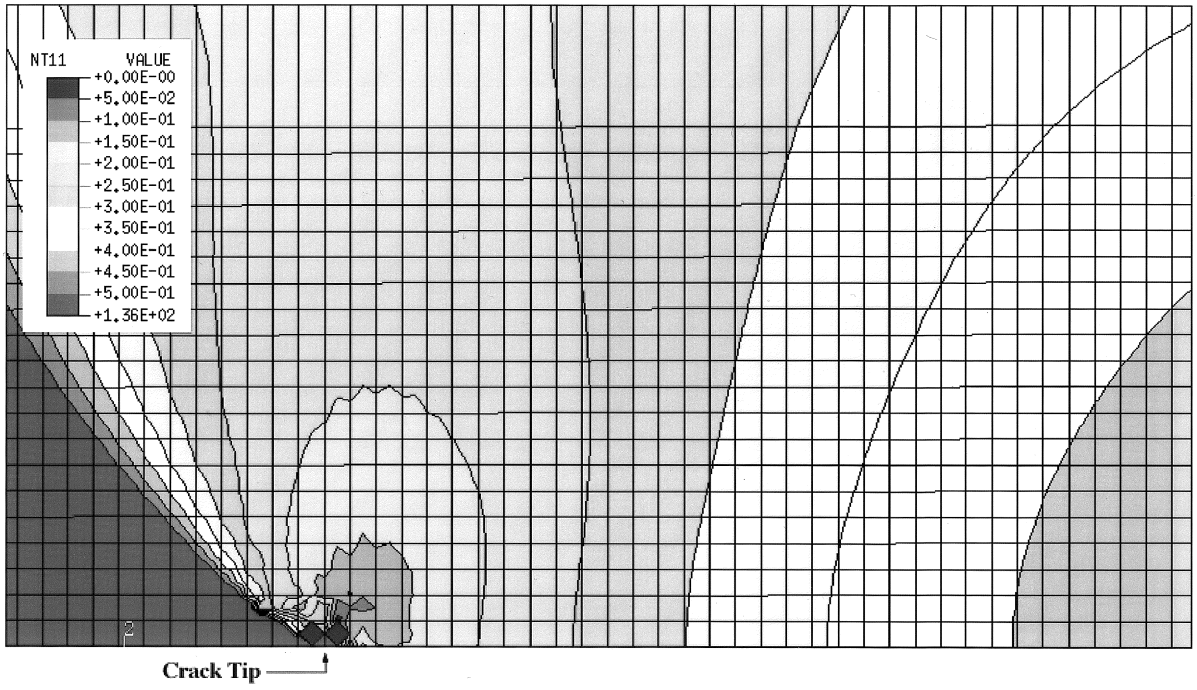

Fig. 10. Contours illustrating the extent of *K*-dominance, through quantity e_2, for a cracked 60-h irradiated ECO sheet with a crack length of (a) 30 mm and (b) 44 mm.

two devices has its own time scale and the two must be synchronized. The error involved in this synchronization was less than 1 s for the experiments conducted. Since in a typical experiment crack initiation occurs 2000 s after the beginning of loading, this error was considered negligible except at the moment when the crack became unstable. The CCD camera provides individual images of the specimen at a maximum rate of 60 frames per second. Thus crack initiation can at best be bracketed by two neighboring frames. However, it is extremely difficult to pinpoint the two frames between which the crack initiation has occurred. In our experiments it was estimated that the error in refining the initiation time in some cases may be as high as 10 s. However, the applied load (Fig. 4), and thus K_{IC}, did not vary much in the interval under consideration.

3. Fracture behavior of FGMs

3.1. FGM fabrication technique

In Lambros et al. (1999) the authors developed a simple and inexpensive way to fabricate laboratory sized FGMs that can be used to conduct fracture tests. For the sake of completeness a brief description of the fabrication process is discussed here. The reader is referred to Lambros et al. (1999) for more details. Fabrication of the FGM is based on the phenomenon that polyethylene co-carbon monoxide (ECO) undergoes property changes when subjected to UV irradiation. It was seen by Lambros et al. (1999) that uniformly irradiated ECO material becomes stiffer, stronger and more brittle with increasing irradiation time. Young's modulus increases from about 160 MPa to about 250 MPa while the strain to failure decreases from a maximum of about 900% to under 10% after about 100 h of UV irradiation. The failure stress and yield stress also increased, in general, with the increasing irradiation time.

In our method of model FGM fabrication, we use a shield to block the UV light from irradiating the ECO specimen. By uncovering the shield gradually, we can control the UV irradiation time of different parts of the specimen and thus gradually change the mechanical properties of the ECO specimen. The FGMs synthesized in this way have properties varying in-plane and can therefore have dimensions on the order of the size of the UV source. In addition, the FGMs thus constructed are truly continuous as opposed to elaborate layered structures and may be used with greater confidence in the experimental verification of existing theoretical models. A typical variation of Young's modulus versus width in an FGM specimen thus constructed is shown in Fig. 11.

3.2. Testing of FGMs

In this section we describe the fracture tests of single edge notch FGM sheets. We obtain the fracture parameters for these FGMs through a similar hybrid numerical-experimental method to that previously developed for homogeneous ECO and described in Section 2.

The fracture test specimen for the FGM sheet has the same dimensions and uses the same loading mechanism as the homogeneous ECO fracture specimen. Experiments were conducted with a 30 mm pre-crack, residing in either the brittle or the ductile side of the FGM. However, it was seen that when the starter crack was in the ductile region, crack growth rapidly became unstable, even at the slowest crosshead speed (0.05 mm/min). Such behavior is expected from an FGM, and has been predicted theoretically, although experimental verification was lacking until this point. All subsequent experiments described in this paper have the pre-crack in the brittle side of the FGM to avoid this problem. Fig. 12 shows typical load versus crack length results for a single edge notch FGM fracture experiment. The variation of Young's modulus for this specific sample is presented in Table 1.

The significance of FGMs is in the nature of their material inhomogeneity. Thus, in the FEA we

attempt to simulate this inhomogeneity as closely as possible. The geometry of the FEA model was the same as in the homogeneous case (Fig. 5). Once again, symmetry was used and the experimentally recorded load and crack length values were input as boundary conditions at each time instant. We meshed the model in such a way that it can be divided evenly into 15 columns. We then assigned different properties to each of the columns, thus creating a graded material.

It is well known that for a homogeneous elastic material, the J-integral is path independent (Rice, 1968). However, this is not the case for a nonhomogeneous material such as an FGM. Therefore, use of the traditional J-integral for characterizing the fracture of an FGM is not appropriate. A modified J-integral, that is path independent in the inhomogeneous material case, has been developed by Aoki et al. (1981), but would require considerable analysis before implementation here. Thus, to circumvent the awkward use of the J-integral in the FGM case, we compute the energy release rate G by a node release method identical to the one used for the homogeneous materials. Fig. 14 shows a comparison of G versus crack length for the 5-, 60- and 106-h homogeneously irradiated ECO and the result for a typical nonhomogeneous material, FGM no. 5. The curves for the three homogeneous materials are identical to those in Fig. 6. In all cases the initial crack length was 30 mm. In our window of observation for FGM No. 5, the crack length reached approximately 70 mm length. Such growth corresponds to movement of the crack tip between zones irradiated at 111 and 71 h. It can be seen that fracture resistance of the homogeneous ECO increases after initiation and then stays approximately constant, with the curves flattening out as irradiation time increases. Contrary to this behavior, G for the FGM constantly increases, and in fact with the opposite curvature of that in the homogeneous materials, indicating the possibility of continued toughening even for crack growth past the window of observation of the present experiments.

At the beginning stages of crack propagation, the crack tip of the FGM specimen resided in a region with about the same property as that of a 106-h uniformly irradiated ECO. As the crack grew into the less irradiated region, since the Young's modulus decreased and strain to failure increased, the material became stronger and more ductile. Consequently G increased. This shows that the FGM can exhibit a

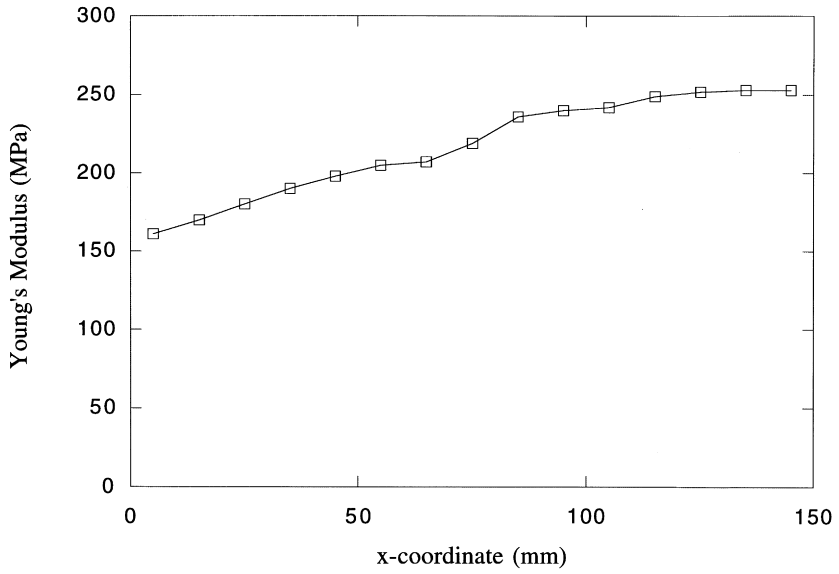

Fig. 11. Typical variation of Young's modulus versus distance for a model FGM sample.

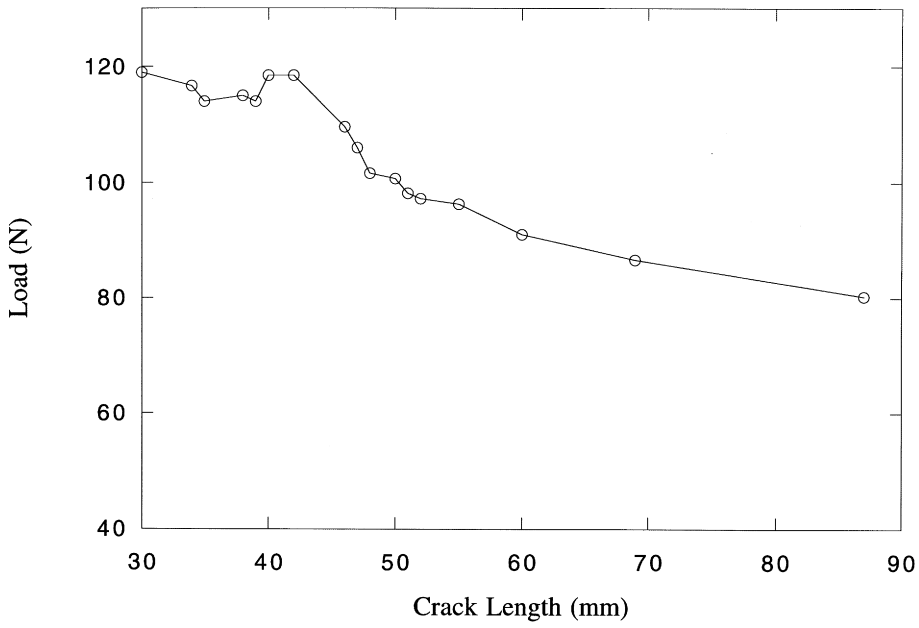

Fig. 12. Experimentally measured load versus crack length relation for FGM edge crack specimen.

significant built-in resistance curve, or R-curve, behavior in crack propagation. This phenomenon is important since the driving force must increase to maintain crack growth.

The stress intensity factor for the FGM can be determined through the relation

$$G = \frac{K_{\mathrm{I}}^2}{E_{\mathrm{tip}}}, \tag{6}$$

Table 1
Typical variation of Young's modulus with distance for FGM specimen

X-coordinate (mm)	Young's modulus (MPa)
5	161
15	170
25	180
35	190
45	198
55	205
65	207
75	219
85	236
95	240
105	242
115	249
125	252
135	253
145	253

where E_{tip} is the Young's modulus at the current location of the crack tip (Jin and Batra, 1996). For completeness, Fig. 14 shows the corresponding stress intensity factors K_I of the uniformly irradiated ECO [from eqn (3)] and FGM No. 5 [from eqn (6)]. Similar behavior to that of Fig. 13 is observed. The results for the stress intensity factor can be compared with the theoretical solution of Erdogan and Wu (1997). In their work, Erdogan and Wu (1997) solve the problem of an edge cracked FGM plate subjected to either an applied displacement or an applied moment. The loading apparatus used in the present study (Fig. 1) can be considered as providing a combination of the two. The results from the FEA can be used to estimate the uniaxial strain and the moment applied to the fracture specimen. The applied displacement is considered to be the displacement of the midpoint of the specimen's upper surface. The applied moment can be easily calculated by the nodal forces and moment arms obtained from the FEA. Thus, since the problem is linear, the theoretical stress intensity factor for the FGM can be easily obtained from the addition of the contribution of the parts from the applied strain and the applied moment. For the case of FGM No. 5, at the instant of crack initiation, the experimentally measured $K_{IC} = 0.647$ MPa$\sqrt{}$m and the value predicted by Erdogan and Wu (1997) solution is $K_{IC} =$ 0.734 MPa$\sqrt{}$m. The two values are 12% different, possibly because of the errors in experimentally determining K_{IC} and the fact that the Erdogan and Wu (1997) solution assumes plane strain conditions, unlike the experiments conducted here.

The procedure used to obtain G and K_I for the FGM material has the same limitations as those described in Section 2.4. Nonetheless, the preliminary experimental results obtained in this study show that FGMs do exhibit a significant built-in resistance curve behavior, a fact that has been theoretically speculated in the past but never been experimentally verified. Such resistance behavior has important design implications, as it would allow for precise tailoring of the response of a structure to unwanted fracture.

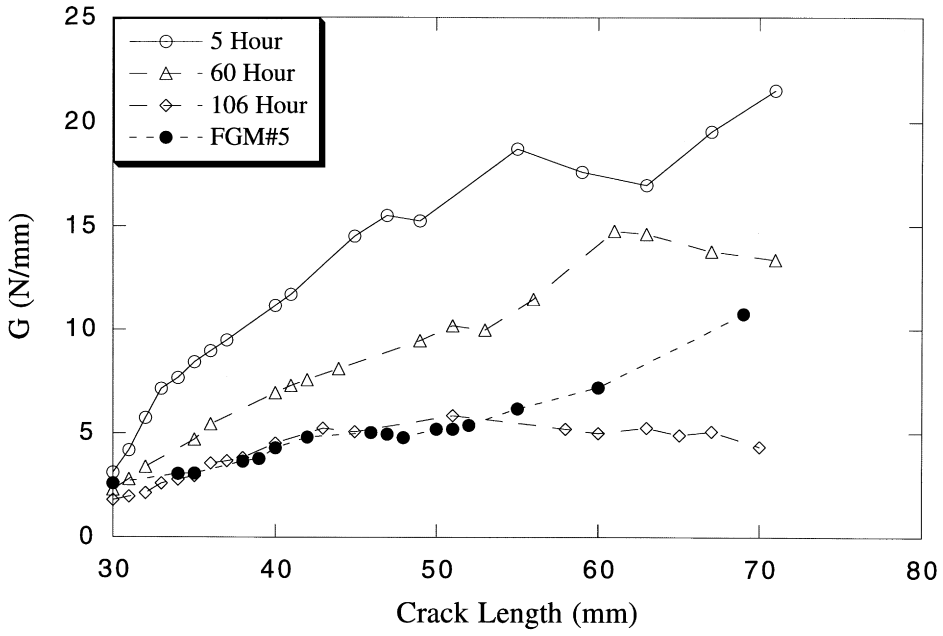

Fig. 13. Comparison of the energy release rate G resistance curves for an FGM and for homogeneous ECO specimens at 5-, 60- and 106-h irradiation.

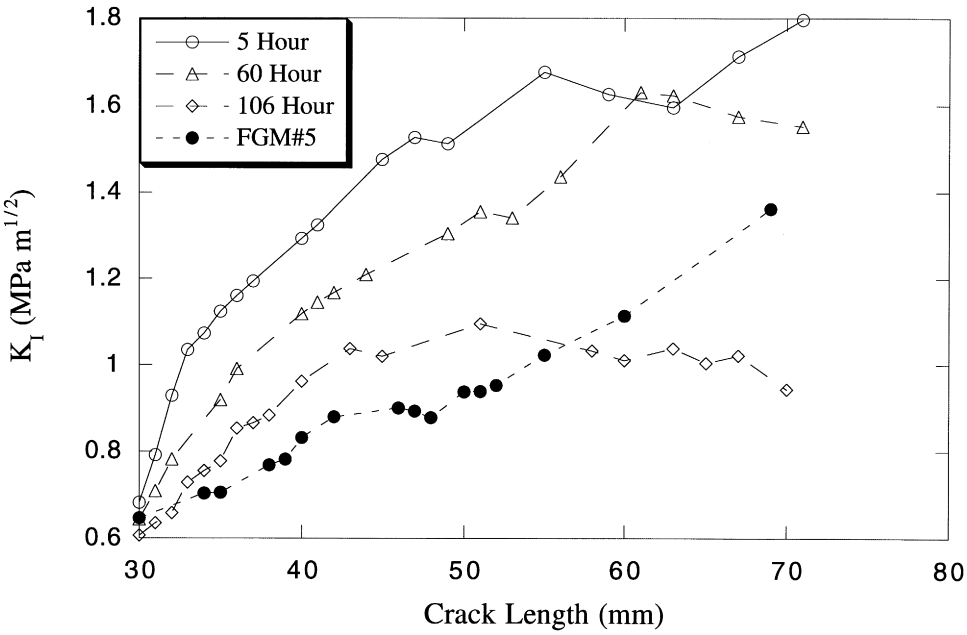

Fig. 14. Comparison of the stress intensity factor K_I resistance curves for an FGM and for homogeneous ECO specimens at 5-, 60- and 106-h irradiation.

4. Conclusions

In this paper we have studied the fracture characteristics of homogeneously UV irradiated ECO as well as model Functionally Graded Materials based on ECO irradiation. With the aid of a CCD camera, a digital storing oscilloscope and an SGI computer, we obtained the load versus crack length relation in fracture experiments of ECO, which we used as input to a finite element analysis. By the FEA method we calculated the fracture parameters J and energy release rate, G, which were then used to compute the stress intensity factor K_I. The toughness of uniformly UV irradiated ECO experienced an initial rise corresponding to crack initiation and blunting, remained constant for a while and then decreased during the crack growth. In addition, its magnitude decreased with increasing irradiation time, which indicated that the material was becoming less ductile.

Using the same experimental setup as developed for the homogenous ECO fracture tests and applying the same loading conditions, we obtained the load versus crack length relation, which was used as boundary and load conditions in the FEA of the FGM. We also assigned the experimentally measured graded material properties into evenly distributed element columns in the FEA model. The concepts of energy release rate and stress intensity factor can also be applied to FGMs to determine their fracture resistance. Our experimental results showed that the fracture behavior of the homogeneous ECO material and the ECO based FGM have significant differences. In contrast to the homogeneously irradiated ECO, the fracture toughness of the FGM in our experiments kept increasing as the crack initiated from the brittle area and grew into the ductile area. When the pre-crack of the FGM specimen was located in the brittle side, the FGM showed a built-in fracture resistance behavior implying that it requires increased driving force to sustain crack growth.

Acknowledgements

Funding for this research has been provided by the National Science Foundation (grant CMS-9712831). We also wish to thank Hi-Cone Division of Illinois Tools Work Co., and especially Mr. Craig Arends V.P. of Engineering and Packaging, for providing the testing material, ECO, for our research free of charge.

References

Andrady, A.L., Nakatsuka, S., 1994. Studies on enhanced degradable plastics III—The effect of weathering of polyethylene and ethylene–carbon monoxide copolymers on moisture and carbon dioxide permeability. Journal of Environmental Polymer Degradation 2 (2), 161–167.

Aoki, S., Kishimoto, K., Sakata, M., 1981. Crack-tip stress and strain singularity in thermally loaded elastic–plastic material. Journal of Applied Mechanics 48, 428–429.

Atkinson, C., List, R.D., 1978. Steady state crack propagation into media with spatially varying elastic properties. International Journal of Engineering Science 16, 717–730.

Choi, H.J., 1996. An analysis of cracking in a layered medium with a functionally graded nonhomogeneous interface. Journal of Applied Mechanics 63 (2), 479–486.

Delale, F., Erdogan, F., 1983. The crack problem for a nonhomogeneous plane. Journal of Applied Mechanics 50, 609–614.

Delale, F., Erdogan, F., 1988a. Interface crack in a nonhomogeneous elastic medium. International Journal of Engineering Science 26 (6), 559–568.

Delale, F., Erdogan, F., 1988b. On the mechanical modeling of the interfacial region in bonded half-planes. Journal of Applied Mechanics 55, 317–324.

Domininghaus, H., 1993. Plastics for Engineers: materials, properties and applications. Hanser, Munich, Germany.

Erdogan, F., 1995. Fracture mechanics of functionally graded materials. Composites Engineering 5 (7), 753–770.

Erdogan, F., Wu, B.H., 1997. The surface crack problem for a plate with functionally graded properties. Journal of Applied Mechanics 64, 449–456.

Gao, X., Kuang, Z.B., 1992. Mode I fracture in two dissimilar functional nonhomogeneous planes. Engineering Fracture Mechanics 42, 33–44.

Gerasoulis, A., Srivastav, R.P., 1980. A Griffith crack problem for a nonhomogeneous medium. International Journal of Engineering Science 18, 239–247.

Ivanova, E., Chudnovsky, A., et al., 1995. The effect of UV radiation on fatigue behavior of polymers. In: Proceedings of ANTEC 95, 3893–3897.

Ivanova, E., Chudnovsky, A., et al., 1996. A new experimental technique for modeling of a micro-heterogeneous media. Experimental Techniques 20 (6), 11–13.

Jin, Z.H., Batra, R.C., 1996. Some basic fracture mechanics concepts in functionally graded materials. Journal of the Mechanics and Physics of Solids 44 (8), 1221–1235.

Jin, Z.H., Noda, N., 1994. Crack-tip singular fields in nonhomogeneous materials. Journal of Applied Mechanics 61 (3), 738–740.

Konda, N., Erdogan, F., 1994. The mixed mode crack problem in a nonhomogeneous elastic medium. Engineering Fracture Mechanics 47 (4), 533–545.

Lambros, J., Santare, M.H., Li, H., Sapna, G.I., 1999. A novel technique for the fabrication of laboratory scale Model Functionally Graded Materials. Experimental Mechanics 39(3), 184–190.

Li, S.K., Guillet, J.E., 1980. Photochemistry of ketone polymers. XIV: Studies of ethylene copolymer. Journal of Polymer Science: Polymer Chemistry Edition 18, 2221–2238.

Rabin, B.H., Shiota, I., 1995. Functionally graded materials. Materials Research Society Bulletin 20 (1), 14–18.

Rosakis, P., Rosakis, A.J., 1988. The screw dislocation problem in incompressible finite elastostatics: a discussion of non-linear effects. Journal of Elasticity 20, 3–40.